Nonparametric probabilistic approach for uncertainty quantification of geometrically nonlinear mistuned bladed-disks

Evangéline Capiez-Lernout, Christian Soize

Nonparametric probabilistic approach for uncertainty quantification of geometrically nonlinear mistuned bladed-disks.

Evangéline Capiez-Lernout, Christian Soize

Université Paris-Est, Laboratoire Modélisation et Simulation Multi-échelle, MSME UMR 8208 CNRS, 5 bd Descartes, 77454 Marne-la-Vallée Cedex 02, France

E-mail: evangeline.capiez-lernout@u-pem.fr

E-mail: christian.soize@u-pem.fr

Abstract. The present research concerns the dynamical analysis of mistuned rotating bladed-disks for which nonlinear geometrical effects exist. The present methodology requires the construction of an adapted reduced-order basis from which a nonlinear reduced-order model is constructed. The mistuning phenomenon is taken into account by considering a nonparametric probabilistic approach based on the information theory. In the present context the uncertainty is introduced by replacing the reduced-order basis with a stochastic reduced-order basis (SROB). This latter one is obtained by using a new nonparametric probabilistic approach of model-form uncertainties so that each realization of the SROB respects some mathematical properties linked to the available information under constraints concerning the specified boundary conditions and the usual orthogonality properties. With such strategy, the computational effort is focused on the stochastic nonlinear reduced internal forces and the related tangential operator which are explicitly constructed using the SROB combined with the finite element method. The numerical application is a rotating mistuned bladed-disk subjected to a load for which geometrical nonlinearities effects occur. The uncertainty propagation in this nonlinear dynamical system is then analyzed.

1. Introduction

Nowadays, a main challenge in engineering structural dynamics concerns the development of computational strategies for constructing stochastic nonlinear reduced-order models that are able to accurately reproduce dynamical structural responses that occur in nonlinear vibrational operating ranges. On one hand, a particular attention has to be paid on the construction of nonlinear deterministic reduced-order models [1, 2, 3, 4, 5], that have to be compatible with non intrusive computational strategies regarding existing industrial softwares. On the other hand, uncertainties can be implemented from the mechanical or geometrical parameters of a given deterministic computational model or with nonparametric probabilistic approaches, which are parameterized by hyperparameters directly linked to the considered reduced-order models. We are interested in this latter strategy that allows both model and parameter uncertainties to be considered. In previous researches, uncertainty was introduced from the nonlinear reduced-operators issued from a given mean reduced-order model [6, 2, 7]. With the proposed method, the uncertainty is introduced by replacing the deterministic reduced-order basis with a stochastic reduced-order basis. This latter one is obtained by using a new nonparametric probabilistic approach [8, 9] so that each realization of the random projection basis respects some mathematical properties linked to the available information. Moreover, it is parameterized by a small number of hyperparameters. It is then used as the projection basis for constructing the stochastic nonlinear reduced-order model. With such uncertainty modeling, the numerical effort is focused on the construction of the stochastic nonlinear reduced internal forces, which is explicitly carried out using the stochastic reduced-order basis combined with the finite element method. The paper is organized as follows. In Section 2, the computational methodology is described. In particular, the computation of the mean nonlinear dynamical finite element response is used for constructing an adapted reduced-order basis with the proper orthogonal decomposition method. The stochastic nonlinear computational model is then written and the main steps concerning the computational resolution of the set of stochastic nonlinear differential equations are discussed. Section 3 is devoted to a numerical application consisting in a rotating bladed-disk structure for which the uncertainty propagation of the nonlinear dynamical response is analyzed in detail.

2. Description of the methodology

2.1. Context of the method

This research concerns the propagation of uncertainties through structural elasto-dynamical systems with finite displacements. In such a context, a complete methodology has already been developed and a dedicated numerical tool that is adapted for large numerical computational models and that is non intrusive with respect to the industrial softwares has been constructed [2, 10, 7]. More specifically, the mistuning analysis of bladed-disks that undergo large strains/displacements has been considered in [7]. In this case, the model used for taking into account mistuning uncertainties has been issued from the nonparametric probabilistic approach for which a dedicated probability model issued from the maximum entropy principle has been directly implemented on the reduced operators of a mean nonlinear reduced-order model [11]. With the presence of geometric nonlinearities, this strategy requires

(i) the knowledge of all the linear, quadratic and cubic stiffness operators of a deterministic nonlinear reduced-order model that can be obtained for instance by judiciously exploring the indirect use of industrial softwares to get all these linear, quadratic and cubic stiffness contributions [3] or in the present case by explicit construction with the finite element method [2].

(ii) the construction of a positive stiffness operator whose entries are all the linear, quadratic and cubic stiffness contributions.

(iii) the construction of the corresponding random stiffness operator whose thanks to the nonparametric probabilistic theory defined in [11] combined with a strategy for reducing the size of the random germ [12].

(iv) the extraction of the different random entries in order to compute the stochastic reduced nonlinear forces and the corresponding stochastic tangent operator. The first one is required by the computational algorithms that are used for solving the stochastic nonlinear differential equations. It should be noted that the use of the latter one depends on the nonlinear algorithm used (Newton or arc-length based).

In the present context, a nonparametric probabilistic approach on the model-form recently introduced in [8] is considered. This paper presents a first attempt for evaluating this new method in the context of turbomachinery mistuning. Such strategy requires

(i) the knowledge of a deterministic reduced-order basis that is used for constructing a deterministic nonlinear reduced-order model for which the reduced quadratic and cubic stiffness do not need to be constructed.

(ii) the construction of a stochastic reduced-order basis by using this new nonparametric approach of model-form uncertainties.

(iii) the explicit construction of the stochastic reduced nonlinear internal forces and its corresponding stochastic tangential operator by using the finite element method. Note that such construction is carried out for each finite element and that the assemblage is performed with a summation over each finite element.

As a consequence, the computational strategy has strongly been modified with respect to the previous researches and has therefore to be adapted. Below, the main steps of this new methodology are summarized, the related novel developments are explained and the advantages and drawbacks are pointed out.

2.2. Mean nonlinear finite element model of the structure

The structure under consideration is a bladed-disk structure with a M-order cyclic symmetry that rotates around its symmetry axis with constant angular speed Ω. The dynamical equations are expressed in the rotating frame of an equilibrium configuration. The structure is assumed to be fixed on a part of its boundary (i. e.the disk's inner radius). In the context of the finite element method, the nonlinear finite element computational model that describes the nonlinear dynamical forced response of the considered structure is characterized in the time domain by the following set of nonlinear coupled differential equations such that

$$[\underline{M}]\ddot{\underline{\mathbf{U}}}(t) + ([\underline{D}] + [\underline{C}_G(\Omega)])\dot{\underline{\mathbf{U}}}(t) + [\underline{K}(\Omega)]\underline{\mathbf{U}}(t) + \underline{\mathbf{F}}^{\mathrm{NL}}(\underline{\mathbf{U}}(t)) = \underline{\mathbf{F}}(t) \quad , \tag{1}$$

$$[\underline{B}]^T\,\underline{\mathbf{U}}(t) = \mathbf{0} \tag{2}$$

in which the $\mathbb{R}^n$-vector $\underline{\mathbf{U}}(t)$ is the instantaneous displacement vector. In Eq. (2), the real matrices $[\underline{M}]$, $[\underline{D}]$ and $[\underline{K}(\Omega)]$ are the mass, damping, and linear stiffness $(n \times n)$ real matrices with symmetry positive definiteness property and the real matrix , $[\underline{C}_G(\Omega)]$ is the gyroscopic coupling matrix with antisymmetry property. The $\mathbb{R}^n$-vector $\underline{\mathbf{F}}(t)$ is issued from the finite element discretization of the external load and the $\mathbb{R}^n$-vector $\underline{\mathbf{F}}^{\mathrm{NL}}(\underline{\mathbf{U}}(t))$ describes the nonlinear finite element internal forces induced by the geometrical nonlinearities. The linear stiffness matrix can be written as

$$[\underline{K}(\Omega)] = [\underline{K}_e] + [\underline{K}_g] + [\underline{K}_c(\Omega)] \quad , \tag{3}$$

in which $[\underline{K}_e]$ represents the elastic stiffness, where $[\underline{K}_g]$ describes the geometric stiffness that is calculated from the stress state of the system submitted to centrifugal loads and where $[\underline{K}_c(\Omega)]$ is the centrifugal stiffness. In Eq. (2), the real $(n \times n_{\mathrm{BC}})$ matrix $[\underline{B}]$ describes the n_{BC} constraint relations defining the Dirichlet conditions, verifying the relation $[\underline{B}]^T[\underline{B}] = [I_{n_{\mathrm{BC}}}]$. Since we are interested in analyzing the nonlinear vibrations of the structure, the external load is defined in the time domain for $t \in \mathbb{R}$ and a Fourier transform with respect to the time domain is performed on the nonlinear solution and allows then the nonlinear dynamical response in the frequency domain to be analyzed. In the present research, it is chosen to solve this set of nonlinear differential equations in order to construct the nonlinear dynamical response that will be considered as the reference response. In this case, the nonlinear algorithms require to construct the nonlinear internal finite element forces and the related tangential operator with the finite element model. Note that such computation is particularly time consuming but is carried out once.

2.3. Construction of the projection basis

The construction of the mean nonlinear reduced-order model requires a projection basis. In the present work, such projection basis is computed from the nonlinear reference response with the proper-orthogonal decomposition method (POD-method), which is proved to be particularly relevant for nonlinear problems. Let $[\underline{A}]$ be the $(n \times n)$ correlation matrix related to the nonlinear reference dynamical response $\underline{\mathbf{U}}(t)$. It is defined by

$$[\underline{A}] = [\mathbb{Y}]^T \, [\mathbb{Y}] \quad , \quad [\mathbb{Y}]_{ij} \, = \, \underline{U}_i(t_j) \, \sqrt{\delta \, t} \quad , \tag{4}$$

in which $\delta \, t$ is the constant sampling time step, and where t_j denotes the sampling time number j. The projection basis is defined by the eigenvectors $\underline{\boldsymbol{\varphi}}_\alpha$ related to the N most contributing eigenvalues $\underline{\lambda}_\alpha$, solution of

$$[\underline{A}] \, \underline{\boldsymbol{\varphi}}_\alpha = \underline{\lambda}_\alpha \, \underline{\boldsymbol{\varphi}}_\alpha \quad \text{with} \quad \underline{\boldsymbol{\varphi}}_\alpha^T \, \underline{\boldsymbol{\varphi}}_\beta = \delta_{\alpha\beta} \quad , \tag{5}$$

in which $\delta_{\alpha\beta}$ is the Kronecker symbol set to 1 if $\alpha = \beta$ and to 0 otherwise. Note that in practice, for large computational models, the numerical construction of correlation matrix $[A]$ is difficult to achieve. In such a case, $[\underline{A}]$ is not computed and the eigenvalue problem is replaced by a singular value decomposition of $[\mathbb{Y}]$ or $[\mathbb{Y}]^T$.

2.4. Stochastic nonlinear reduced-order model

In this work, the nonparametric probabilistic approach of model-form uncertainties recently introduced in [8] is used. In such case, the probability model is directly implemented in the projection basis. Let $[\underline{\Phi}]$ be the $(n \times N)$ matrix whose columns are the eigenvectors $\underline{\boldsymbol{\varphi}}_1, \cdots, \underline{\boldsymbol{\varphi}}_N$. The matrix $[\underline{\Phi}]$ is then replaced by a stochastic matrix $[\mathbf{\Phi}(\boldsymbol{\alpha})]$, whose probability model is described in [8]. It should be noted that the random vectors contained in random matrix $[\mathbf{\Phi}]$ statisfy the boundary conditions and orthonormality conditions

$$[\underline{B}]^T [\mathbf{\Phi}] = \mathbf{0} \quad , \quad [\mathbf{\Phi}]^{\mathbf{T}} [\mathbf{\Phi}] = [\mathbf{I_N}] \quad , \tag{6}$$

in which $[I_N]$ is the identity matrix with N order. The probability distribution of random matrix $[\mathbf{\Phi}]$ depends on a $\mathbb{R}^m$-valued hyper-parameter $\boldsymbol{\alpha} = \{s, \beta, [\sigma]\}$, whose dimension $m = 0.5N(N+1) + 2$ has been optimized according to the modeling. More specifically, s is a scalar, which controls the statistical fluctuations around each deterministic vector basis, β is a scalar that controls the correlation between the components of the vector basis, and $[\sigma]$ is an $(N \times N)$ real upper triangular matrix, which allows for controlling the correlations between the column vector basis. The Monte Carlo numerical procedure for generating such random basis is briefly given below:

$$[\mathbf{\Phi}] \;=\; \Big([\underline{\Phi}] + s[\mathbf{Z}]\Big)\Big([I_N] + s^2\,[\mathbf{Z}]^T\,[\mathbf{Z}]\Big)^{-1/2} \tag{7}$$

$$[\mathbf{Z}] \;=\; [\mathbf{A}] - \frac{1}{2}[\Phi]\Big([\underline{\Phi}]^T[\mathbf{A}] + [\mathbf{A}]^T[\underline{\Phi}]\Big) \tag{8}$$

$$[\mathbf{A}] \;=\; [\mathbf{U}] - [\underline{B}]\Big([\underline{B}]^T[\mathbf{U}]\Big) \tag{9}$$

$$[\mathbf{U}] \;=\; [\mathbf{G}(\beta)][\sigma] \quad , \tag{10}$$

in which $[\mathbf{G}(\beta)]$ is a $(n \times N)$ random matrix whose random generator can be found in details in [8].

The stochastic computational model consists then in solving the set of stochastic nonlinear differential equations

$$[\boldsymbol{\mathcal{M}}]\ddot{\mathbf{Q}}(t) + ([\boldsymbol{\mathcal{D}}] + [\boldsymbol{\mathcal{C}}_G(\Omega)])\,\dot{\mathbf{Q}}(t) + [\boldsymbol{\mathcal{K}}(\Omega)]\mathbf{Q}(t) + [\mathbf{\Phi}]^T\underline{\mathbf{F}}^{\rm NL}([\mathbf{\Phi}]\,\mathbf{Q}(t)) = [\mathbf{\Phi}]^T\underline{\mathbf{F}}(t) \quad , \tag{11}$$

in which $[\boldsymbol{\mathcal{M}}] = [\mathbf{\Phi}]^T\,[\underline{M}]\,[\mathbf{\Phi}]$, $[\boldsymbol{\mathcal{D}}] = [\mathbf{\Phi}]^T\,[\underline{D}]\,[\mathbf{\Phi}]$, $[\boldsymbol{\mathcal{C}}_G(\Omega)] = [\mathbf{\Phi}]^T\,[\underline{C}_G(\Omega)]\,[\mathbf{\Phi}]$ and $[\boldsymbol{\mathcal{K}}(\Omega)] = [\mathbf{\Phi}]^T\,[\underline{K}(\Omega)]\,[\mathbf{\Phi}]$ are the full $(N \times N)$ random mass, damping, gyroscopic coupling and stiffness matrices, and where $\mathbf{Q}$ is the $\mathbb{R}^N$-valued random vector of the generalized coordinates from which the $\mathbb{R}^n$-valued random vector of the physical solution $\mathbf{U}$ is reconstructed by

$$\mathbf{U} = [\mathbf{\Phi}]\,\mathbf{Q} \quad . \tag{12}$$

Regarding the numerical computation, the set of these stochastic nonlinear differential equations is solved in the time domain by using the Monte Carlo numerical simulation, using an implicit and unconditionally stable integration scheme (Newmark method with the averaging acceleration scheme). For each sampling time, the nonlinearity is solved iteratively by using either the fixed point method or an arc-length-based algorithm, depending on the nonlinearity rate. Concerning the current strategy, the knowledge of the nonlinear reduced-order internal force vector is required by both nonlinear algorithms whereas the knowledge of the related reduced tangent operator (that is time consuming) is only required by the use of the arc-length-based algorithm. Practically, the contributions of both nonlinear reduced-order internal force and tangent reduced operator induced by each finite element are explicitly constructed with the finite element method. The assemblage over the finite elements is particularly quick because it only requires to sum each of these contributions. A posterior nonlinear dynamical analysis is performed from Eq.(12) in the frequency domain by computing the Fourier transform of the nonlinear dynamical response.

The main advantage of this new method is that it allows for considering general nonlinear dynamical systems for which the operators are not necessarily known. It also constitutes a global approach because there is no need to analyze and decide whether the mass, the damping or the stiffness matrices are random or not. In opposite, the real difficulty arises when considering the inverse problem because the hyperparameter $\boldsymbol{\alpha}$ that has to be identified has a large dimension that increases with the square of the order of the reduced-order model. This latter point requires some further open researches that allows for reducing the size of the hyperparameter and that are not investigated in the present research.

3. Numerical application

The structure under consideration is a bladed-disk structure of order $M = 24$ whose finite element mesh is constructed with hexahedral solid finite elements with 8 nodes and is constituted of 52 290 degrees of freedom. The computational model is issued from [13] for which the boundary conditions have been modified. The structure is in rotation around its revolution axis with a constant velocity $\Omega = 1\,000\,rpm$. Since the nonlinear dynamic analysis is carried out in the rotating frame of the structure, the rigid body motion due to the rotation of the structure corresponds to a fixed boundary condition located at the inner radius of the structure. The bladed-disk is made up of a homogeneous isotropic linear elastic steel material. A Rayleigh damping model is added for the bladed-disk structure such that $[\underline{D}] = \alpha[\underline{M}] + \beta[\underline{K}]$ with $\alpha = 39.27$, $\beta = 1.53 \times 10^{-6}$ such that fundamental natural frequency $\nu_1 = 383\,Hz$ has a critical damping $\xi_1 = 0.01$.

3.1. Description of the excitation

The cyclic symmetry is first used for solving the linear generalized eigenvalue problem related to the tuned rotating bladed-disk. Figure 1 displays the natural frequencies of the tuned structure ν_i with respect to the circumferential wave number h. From this graph, we are interested by the veering corresponding to circumferential wave number $h = 4$ in the frequency band $[2\,500\,,\,3\,200]\,Hz$. As a consequence, the spatial repartition of the external load described by the normalized vector $\mathbb{F}$ is such that an external point load is applied along all directions at the excitation nodes located at the tip of each blades with a constant phase shift $\frac{\pi}{3}$.

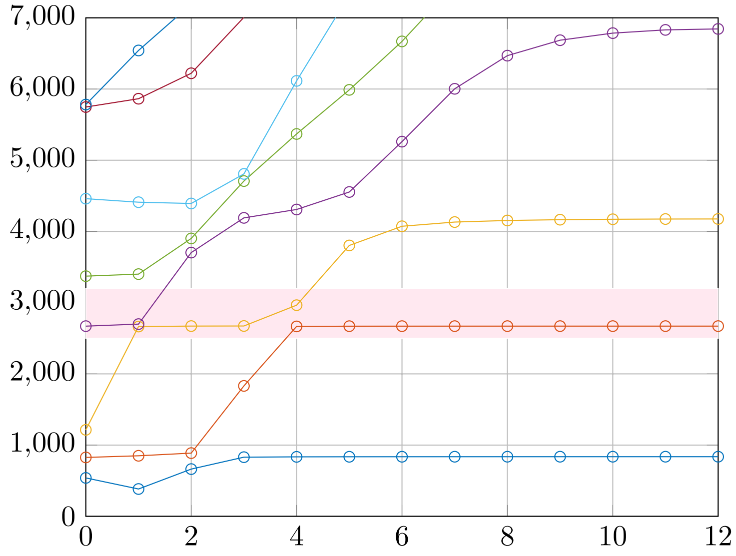

Figure 1. Graph of natural frequencies ν_i with respect to its circumferential wave number h. Excitation frequency band $\mathbb{B}_e$ (light red area)

The time evolution of the load is described by function $g(t)$ allowing for exciting the excitation frequency band $\mathbb{B}_e = [\nu_{\min}\,,\,\nu_{\max}]\,Hz$ represented by the colored pink area and such that $\nu_{\min} = 2\,500\,Hz$ and $\nu_{\max} = 3\,200\,Hz$.

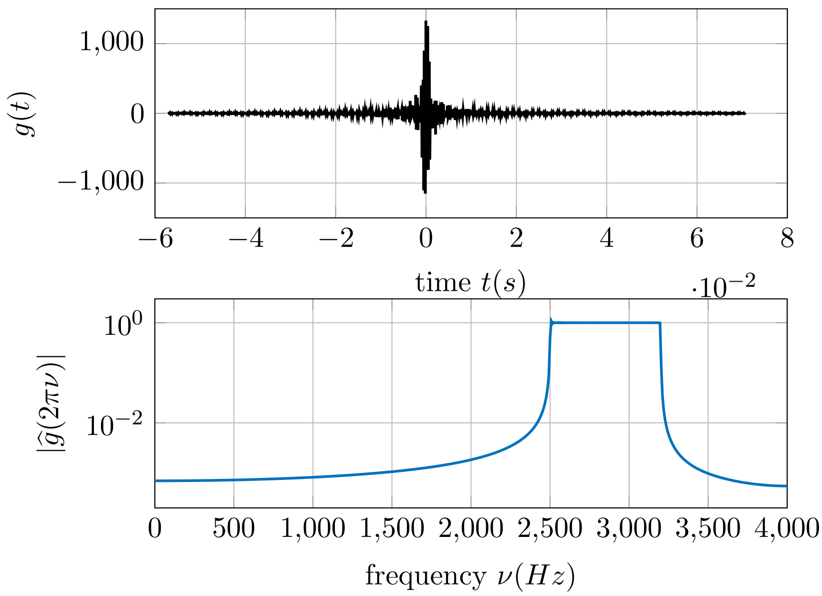

Figure 2. Graph of functions $t \mapsto g(t)$ and $\nu \mapsto |\widehat{g}(2\pi\nu)|$.

In this case, function $g(t)$ is written as

$$g(t) = \frac{2}{\pi\, t} \sin(\pi\, \Delta\nu\, t)\, \cos(2\pi \widetilde{s}\, \Delta\nu\, t) \quad \text{with } \Delta\nu = 700\,Hz\,,\; \widetilde{s} = 4.0714 \quad , \tag{13}$$

such that $|\widehat{g}(2\pi\nu)| = \mathbb{1}_{\mathbb{B}_e}(2\pi\nu)$ as represented in Figure 2. Practically, the computation is carried on a truncated time domain $\mathbb{T} = [t_{ini}, t_{ini} + T]$. The initial load is chosen as $t_{ini} = -0.057\,s$ yielding a null initial load. The time duration T is then adjusted so that the system be returned at its equilibrium state within a given numerical tolerance for both linear and nonlinear computations. Even the fundamental natural frequency does not belong to excitation frequency band $\mathbb{B}_e$, it can be indirectly excited through the geometrical nonlinear effects. Time duration is chosen as $T = 0.128\,s$ which ensures the system to return to its equilibrium state with a relative tolerance $\tau = e^{-2\pi\xi_1\nu_1 T} = 4.6\%$ when fundamental natural frequency is excited. The sample frequency ν_e and the number of time steps are then chosen as $\nu_e = 8\,000\,Hz$ and $n_t = 1\,024$ yielding a constant sampling time step $\delta t = 1.25 \times 10^{-4}\,s$ and a constant sampling frequency step $\delta\nu = 3.907\,Hz$.

Finally, the external loading can be written as

$$\mathbf{F}(t) = s_0\, g(t)\, \mathbb{F} \quad , \tag{14}$$

in which s_0 is the load intensity. In the present case, the case $s_0 = 28.184\,N$ is investigated and corresponds to the case in which geometrical nonlinearities deeply affect the vibrational behavior of the bladed-disk structure.

3.2. Computational results

In this section, the nonlinear finite element response described in Eqs. (2) and(2) is computed and taken as a reference response in the frequency band of analysis $\mathbb{B}_a = [350\,,\,4000]\,Hz$. Such nonlinear reference response is then used in order to construct the projection basis as explained in Section 1. A convergence analysis is then performed in order to set the optimal order of the reduced-order model that can accurately reproduce the reference response. In this case, it is shown that the a good agreement is obtained with $N = 42$. The computational results are presented for $s \in \{0.01, 0.0125, 0.015, 0.0175\}$, $\beta = 0.0025$ and $[\sigma]$ an upper triangular matrix with N order for which the non-zeros entries are defined by $[\sigma]_{ii} = 10$, $[\sigma]_{i,i+1} = 5$ and $[\sigma]_{i,i+2} = 2.5$. Note that these results corresponds to a weakly mistuned situation for which amplification effects are still moderate when only considering the linear effects. The results are computed with $n_s = 70$ Monte Carlo numerical realizations. Let $u^j_\alpha(t)$ be the displacement at the tip of the blade number j along direction $\mathbf{e}_\alpha$ corresponding to the reference solution. We are then interested by the observation defined by $\widehat{v}(2\pi\nu) = \max_j ||\widehat{u}^j_\alpha(2\pi\nu)||$.

Figures 3, 4, 5, and 6 display for $s = \{0.01, 0.0125, 0.015, 0.0175\}$, the graph of function $\nu \mapsto v(2\pi\nu)$ (black dashed line) and the graph of the confidence region (yellow area) of random function $\nu \mapsto V(2\pi\nu)$ of the observation with a probability level $p_c = 0.95$ related to the nonlinear reduced-order model. In these graphs, the sensitivity of the stochastic nonlinear forced response is analyzed with respect to the uncertainty level. As expected, it can be seen that the structure responds outside $\mathbb{B}_e$. More particularly, the resonance located around 2,100 Hz has similar amplitude to the main resonances located in $\mathbb{B}_e$ and matches well to its deterministic counterpart. The resonance located around 1,000 Hz cannot either be neglected. Its robustness to uncertainty is sensitively weak and a frequency shift is observed with respect to the reference response.

An interesting point concerns the particular unexpected robustness of the main resonances that are located in $\mathbb{B}_e$. In the present case, the structure clearly undergoes significant geometrical nonlinear effects since it responds outside the excitation frequency band. One can see that such effects have a tendency to stabilize the dynamical behaviour in $\mathbb{B}_e$. On the contrary, the resonances issued from the propagation of the geometrical nonlinearities have a weaker response level accompanied by a very low response level. It can be seen as a "linear" dynamical behaviour that is known to be sensitive to mistuning uncertainties.

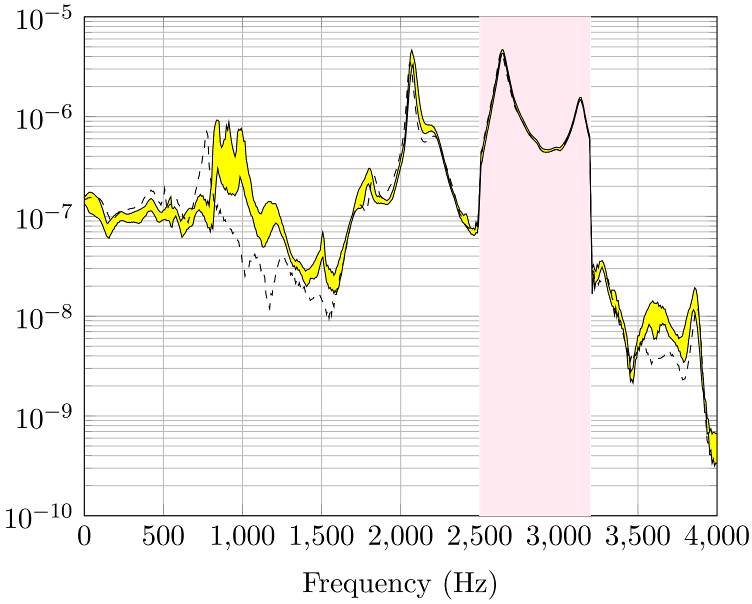

Figure 3. Graph of functions $\nu \mapsto v(2\pi\nu)$ (black dashed line) computed with the deterministic nonlinear finite element model, graph of the confidence region of random function $\nu \mapsto V(2\pi\nu)$ computed with the nonlinear stochastic reduced-order model (yellow area), localization of the excitation frequency band $\mathbb{B}_e$ (light red area) for $s = 0.01$.

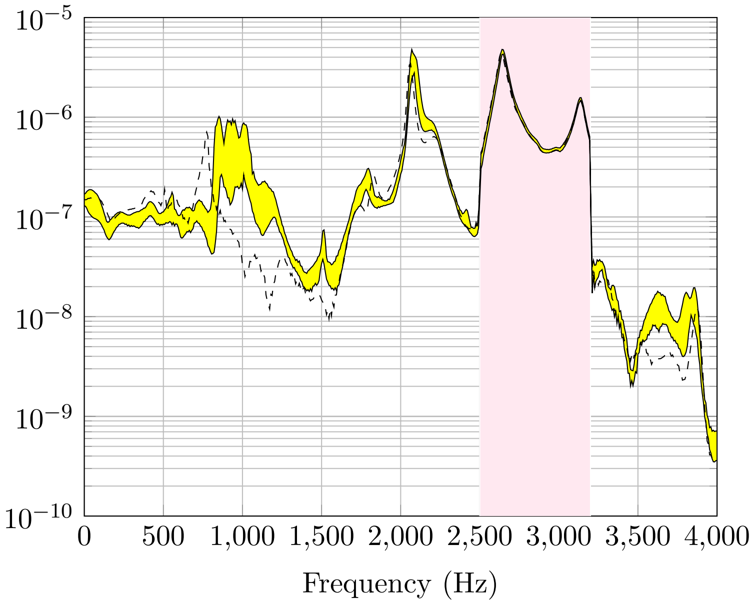

Figure 4. Graph of functions $\nu \mapsto v(2\pi\nu)$ (black dashed line) computed with the deterministic nonlinear finite element model, graph of the confidence region of random function $\nu \mapsto V(2\pi\nu)$ computed with the nonlinear stochastic reduced-order model (yellow area), localization of the excitation frequency band $\mathbb{B}_e$ (light red area) for $s = 0.0125$.

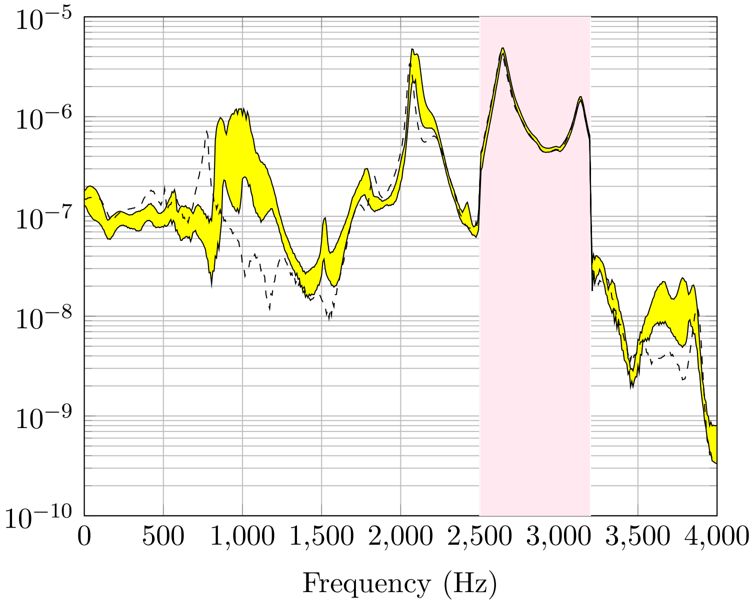

Figure 5. Graph of functions $\nu \mapsto v(2\pi\nu)$ (black dashed line) computed with the deterministic nonlinear finite element model, graph of the confidence region of random function $\nu \mapsto V(2\pi\nu)$ computed with the nonlinear stochastic reduced-order model (yellow area), localization of the excitation frequency band $\mathbb{B}_e$ (light red area) for $s = 0.015$.

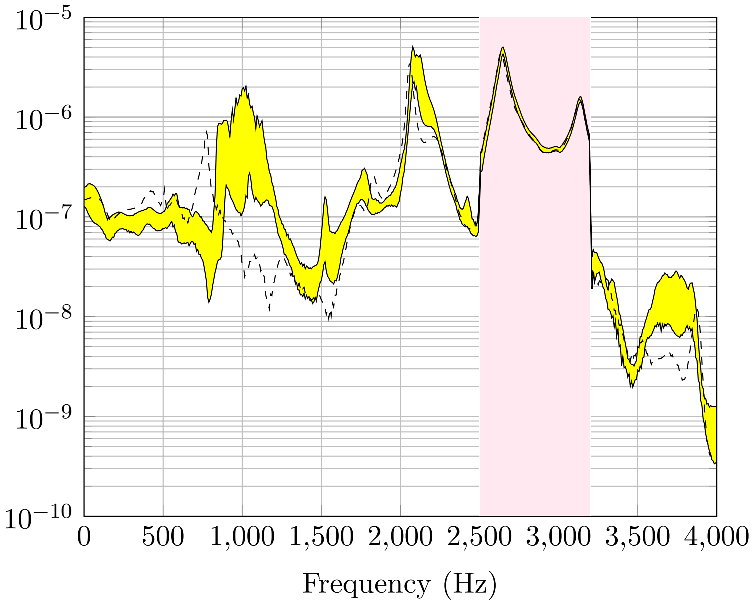

Figure 6. Graph of functions $\nu \mapsto v(2\pi\nu)$ (black dashed line) computed with the deterministic nonlinear finite element model, graph of the confidence region of random function $\nu \mapsto V(2\pi\nu)$ computed with the nonlinear stochastic reduced-order model (yellow area), localization of the excitation frequency band $\mathbb{B}_e$ (light red area) for $s = 0.0175$.

Conclusions

A computational methodology has been presented for analyzing the propagation of uncertainties in the context of structural dynamics with geometric nonlinearities. A nonparametric probabilistic method for modeling model-form uncertainties, which is implemented from a given projection basis is used for constructing a stochastic computational nonlinear reduced-order model . A numerical application, which consists in a rotating bladed-disk structure, is presented and shows the capability of the stochastic computational model to capture the unexpected resonances induced by the geometrical nonlinearities.

Acknowledgement

The authors thanks Pr. Christophe Pierre from the Illinois University concerning the use of the finite element model and also thank Pr. Marc Mignolet from the Arizona State Unversity.

References

[1] Muryavov A and Rizzi S 2003 *Computers & Structures* **81** 1513–1523
[2] Capiez-Lernout E, Soize C and Mignolet M P 2012 *Computational Mechanics* **49** 87–97
[3] M-P Mignolet A Przekop S R and Spottswood M 2013 *Journal of Sound and Vibration* **332** 2437–2460
[4] Gaonkar A and Kulkami S 2013 *Finite Elements in Analysis and Design* **76** 50–62
[5] C Farhat P Avery T C and Cortial J 2014 *International Journal for Numerical Methods in Engineering* **98** 625–662
[6] Mignolet M P and Soize C 2008 *Computer Methods in Applied Mechanics and Engineering* **197** 3951–3963
[7] Capiez-Lernout E, Soize C and Mbaye M 2015 *Journal of Sound and Vibration* **356** 124–143
[8] Soize C and Farhat C 2017 *International Journal for Numerical Methods in Engineering* **109** 837–888
[9] Farhat C, Bos A, Avery P and Soize C 2018 *AIAA Journal* **56** 50–62
[10] Capiez-Lernout E, CSoize and Mignolet M P 2014 *Computer Methods in Applied Mechanics and Engineering* **271** 210–230
[11] Soize C 2012 *Stochastic Models of Uncertainties in Computational Mechanics, Lecture Notes in Engineering Mechanics 2* (American Society of Civil Engineers (ASCE))
[12] Capiez-Lernout E and Soize C 2017 *International journal for Uncertainty Quantification* **7** 83–98
[13] Bladh R, Castanier M and Pierre C 2001 *ASME Journal of Engineering for Gas Turbines and Power* **123** 100–108